P. D. Hobson, M. W. Brown,* and E. R. de los Rios**

Two Phases of Short Crack Growth in a Medium Carbon Steel

REFERENCE Hobson, P. D., Brown, M. W., and de los Rios, E. R. **Two Phases of Short Crack Growth in a Medium Carbon Steel**, *The Behaviour of Short Fatigue Cracks*, EGF Pub. 1 (Edited by K. J. Miller and E. R. de los Rios) 1986, Mechanical Engineering Publications, London, pp. 441–459.

ABSTRACT Many studies of cracks growing under high strain fatigue conditions have revealed growth rates in excess of those predicted by LEFM analyses. In addition, anomalously high growth rates have been measured for very small cracks, of length less than typical microstructural dimensions. Both types of fatigue crack have been classified as 'short'.

An experimental fatigue study using medium carbon steel specimens has shown that both types of crack growth occur. Surface replication enables individual small cracks to be monitored throughout a constant load amplitude test, and their growth rates to be determined. Two equations have been derived, corresponding to each type of short crack growth. These equations calculate the relative proportions of each phase of the fatigue life and therefore they may be used to predict the *S–N* curve for medium carbon steel. The relationship of crack development to microstructural features is also discussed.

Introduction

Although anomalies in the growth of short cracks have been noted for several years (**1**)(**2**), attempts to model such behaviour have only been made recently. The heightened interest in this area of crack growth arises not only from the practical need for increased levels of service stress but also from the inability of established methods of fatigue analysis, such as fracture mechanics, to provide adequate mathematical models. One of the fundamental assumptions in fracture mechanics, that a material is an isotropic continuum, has been shown not to be valid in the case of short crack growth for several materials (e.g., (**3**)–(**5**)) in which microstructural features have been observed to play a dominant role. Using a study of an aluminium alloy (**6**), a crack growth equation has been suggested which incorporates a microstructural dimension to describe the growth of a crack in a single grain (**7**). Combining a general form of this equation together with a second equation to represent crack growth beyond the first grain, it is shown here that the complete history of crack growth for a medium carbon steel may be described adequately.

Experimental work

All fatigue tests were performed in fully reversed tension–compression loading on a servo-hydraulic fatigue testing machine with a load capacity of ±250 kN.

* Department of Mechanical Engineering, University of Sheffield, Mappin Street, Sheffield, UK.

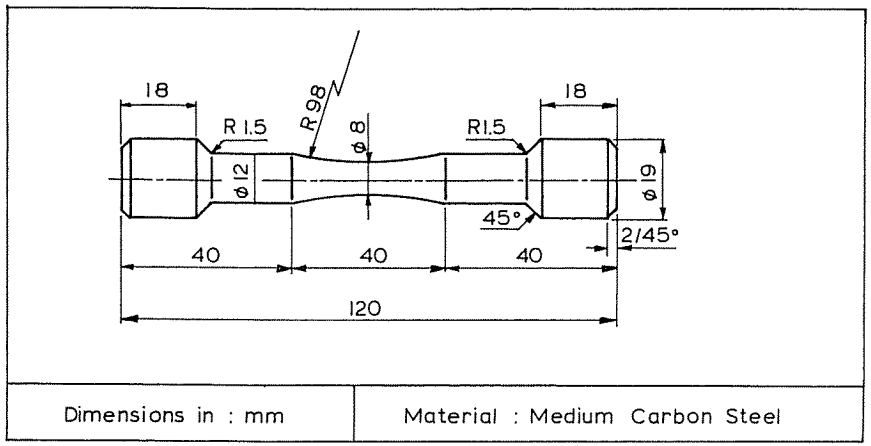

Fig 1 Specimen geometry

The material tested was a medium carbon steel of composition (wt%) 0.4C, 1.0Mn, 0.10Si, 0.001S, 0.005P, with yield and tensile stengths of 392 MPa and 683 MPa, respectively, an elongation to fracture of 44 per cent, and a reduction in area of 36 per cent.

Specimens having a mild hour glass profile were used, as shown in Fig. 1, because this shape limited the area of cracking to the centre of the specimen, thus restricting the region requiring replication to locate cracks. To replicate the surface of the specimen, acetate sheet was softened with the solvent acetone and pressed lightly onto the specimen. For each test, replicas were taken for at least seven stages in life. As most interest was in the growth of short cracks, replicas were taken more frequently during the initial period. Cycling was stopped at maximum tensile load so that the cracks were held open during replication.

Tests with surface replication were performed in load control at stress levels of 998, 816, and 638 MPa, corresponding to lifetimes of approximately 1000, 6000 and 30 000 cycles, respectively. Several tests were carried out at each load range to enable a number of cracks to be studied. A triangular waveform was used at frequencies in the range 0.016–0.3 Hz.

Strain controlled tests were also performed with a diametral extensometer monitoring extension at the minimum diameter of the specimen. Results from all the tests are shown in Figs 2 and 3. In Fig. 2 a least-squares analysis was used for data where $\Delta\sigma > 450$ MPa, in order to model the plastic portion of the cyclic stress–strain curve. Also shown in this figure is the line representing the linear elastic response. The stable cyclic stress–strain curve in Fig. 2 shows both elastic and power law strain-hardening regions in the classical manner, and therefore this behaviour can be adequately represented by the Ramberg–Osgood formulation

$$\Delta\varepsilon = \Delta\sigma/E + (\Delta\sigma/k)^{1/n}$$
$$= \Delta\sigma/203\,000 + (\Delta\sigma/2013)^{1/0.19} \quad (1)$$

Fatigue failure was defined as fracture in load controlled tests, but for strain control a more suitable definition was a 5 per cent decay in the measured load range from the stable level. The diametral extensometer was not used for the load controlled tests as it would have been necessary to remove the extensometer to enable replication of the surface cracks. However, one load controlled experiment was conducted while monitoring the strain to compare with the strain controlled fatigue strength. Figure 3(a) shows that slightly longer life was found for load control, and that the strain controlled life may be found from the Coffin–Manson equation

$$\Delta\varepsilon_p \cdot N_f^{0.673} = 2.23 \quad (2)$$

The *S–N* curve is shown with a stress scale in Fig. 3(b), giving for strain controlled tests the Basquin equation

$$\Delta\sigma \cdot N_f^{0.137} = 2553 \quad (3)$$

The difference in lifetime observed between load and strain controlled tests may be attributed to the choice of failure definition. Assuming that a 5 per cent load decay would correspond to a total crack area of 5 per cent for the low cycle strain controlled tests, and that there are a number of independent fast growing

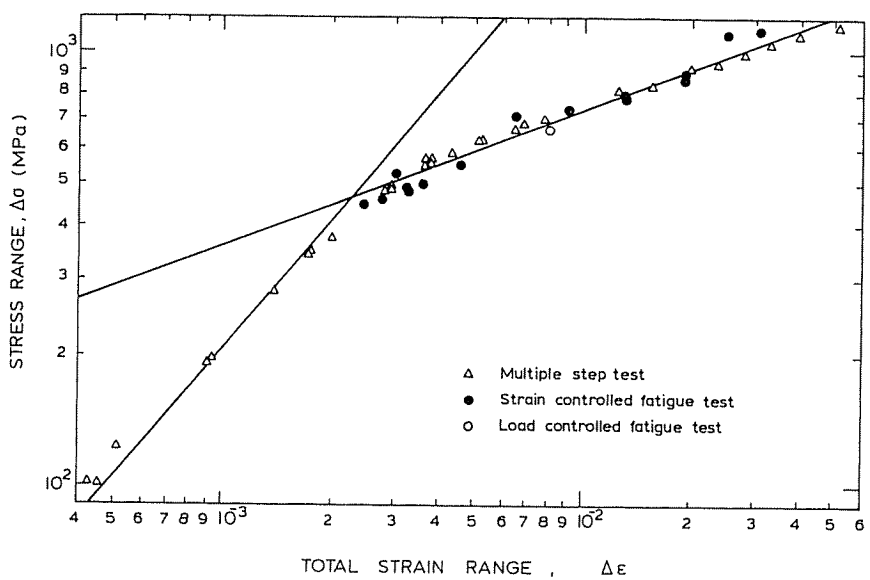

Fig 2 Cyclic stress–strain curve

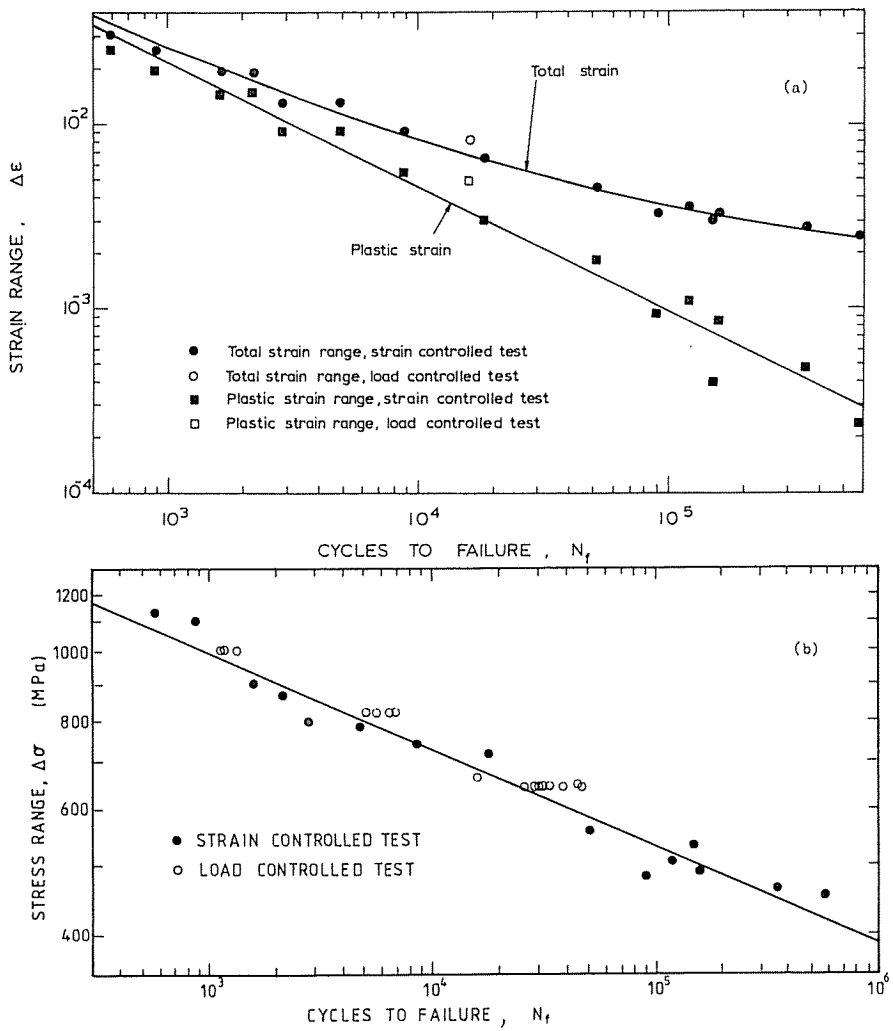

Fig 3 (a) Total and plastic strain life relationships. (b) The *S–N* curve

cracks, say five, of semi-circular shape, then five such cracks correspond to a crack area of $5(\pi R^2/2)$ for cracks of radius R. If 5 per cent of the cross-section is cracked, this must be equal to $(0.05\pi R_1^2)$ where R_1 is the radius of the specimen cross-section, which implies for $R_1 = 4$ mm a value for $2R$ of 1.1 mm for the surface initiation length. This failure crack length will clearly give a reduced endurance compared to the load controlled case where specimen

fracture occurred, which gives a surface crack length of 4 mm required to raise the net section stress to the tensile strength.

Full characterization of the microstructure of this material is given elsewhere (**5**). Briefly it is a typical normalized structure of a 0.4% C steel where the ferrite phase, in the form of long ferrite plates, has formed along the previous austenite grain boundaries. The ferrite plates have an average thickness of 8 μm and an average length of 116 μm. The volume fraction of ferrite is approximately 5 per cent; the rest is pearlite.

Plastic replicas taken from polished and etched specimens showed that cracks initiated in, and grew along, the ferrite plates. Short cracks contained within a single plate exhibited faster growth rates than those that would be predicted by elasto-plastic fracture mechanics. As a crack approached the edge of the ferrite plate that contained the initiation site, the crack growth rate decreased. However, once the crack had extended beyond one ferrite plate it showed a steadily increasing growth rate with subsequent microstructural variations apparently having little effect on it.

This type of growth behaviour is shown in Fig. 4, the plotted data points are surface crack lengths, a_s, obtained during life at the lowest stress level tests, namely 638 MPa. Here the minimum crack growth rate occurred at a crack length of 85 μm after only 6000 cycles out of a life of 29 300 cycles. The growth curve beyond 10 000 cycles conforms with established continuum fracture mechanics predictions, i.e.

$$da/dN = f(\Delta\varepsilon) \cdot a \tag{4}$$

which gives on integration

$$\ln (a) = f(\Delta\varepsilon) \cdot N + A \tag{5}$$

This is a straight line for a constant strain amplitude test, as in Fig. 4. However, for microstructurally short cracks, classical fracture mechanics cannot be employed and a new model for crack propagation must be used.

Theoretical model for microstructural short crack growth

In order to formulate a crack growth equation to model the behaviour of microstructurally short cracks, it is essential to account for microstructural influences. By considering a list of parameters which might be expected to affect the propagation of a crack embedded within the grain containing the nucleation site, a general expression for crack growth may be postulated (**8**), using the method of dimensional analysis

$$da/dN = f(\Delta\sigma, \Delta\varepsilon, E, k, n, \sigma_y, a, d) \tag{6}$$

where f is an unknown function, a is the crack length, σ_y is the yield stress and d is a characteristic dimension representative of the distance between adjacent microstructural obstacles to crack propagation. For stresses greater than yield

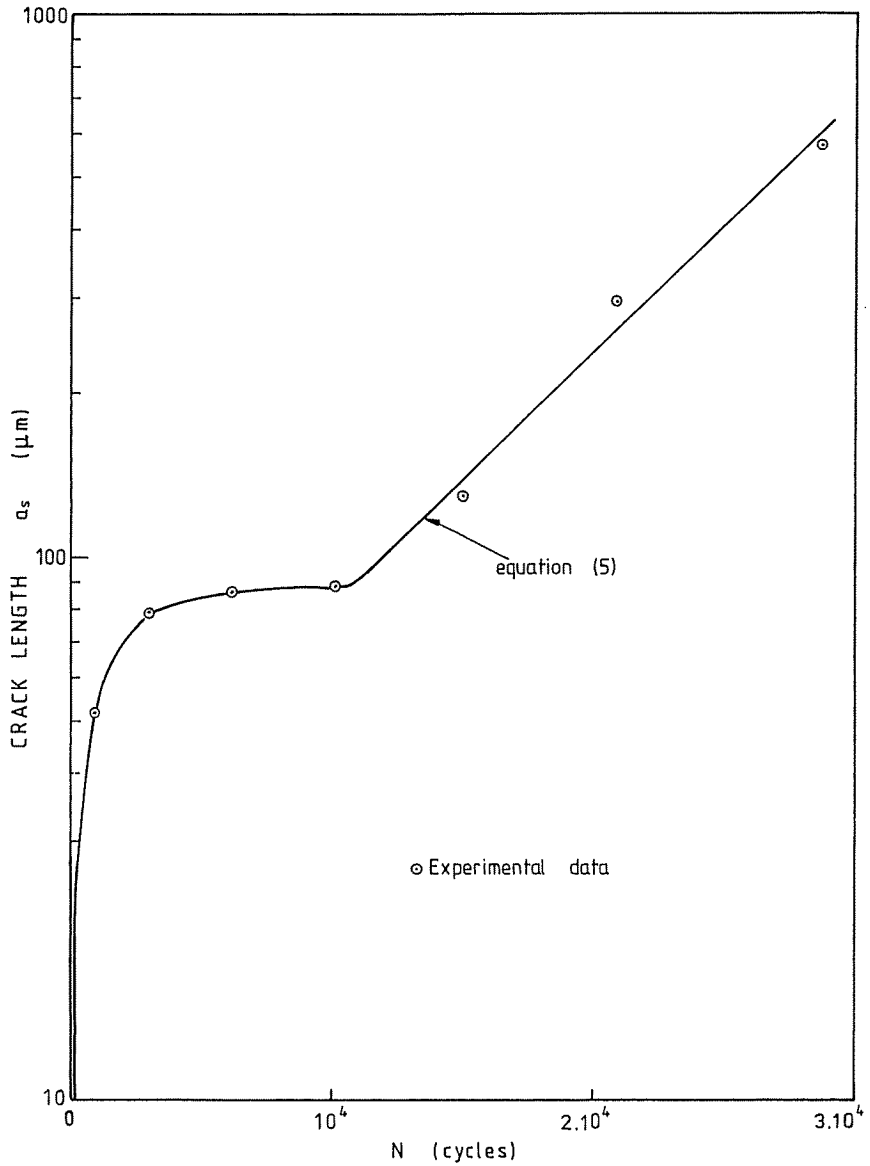

Fig 4 Crack growth curve for one crack with $\Delta\sigma = 638$ MPa, $N_f = 29\,300$

$\Delta\sigma = k\,\Delta\varepsilon_p^n$ as in equation (1), and hence equation (6) includes sufficient parameters to describe the cyclic deformation behaviour of a given material in addition to some microstructural influences. Thus $\Delta\varepsilon$ is a dependent variable and may be excluded from equation (6). The grain size or any other single dominant feature may be represented by the parameter d.

Dividing the left-hand side of equation (6) by a (with $\Delta\varepsilon$ eliminated), and collecting all the quantities into dimensionless groups, one obtains

$$\frac{1}{a}\frac{da}{dN} = f\left(\frac{\Delta\sigma}{k}, \frac{E}{k}, n, \frac{\sigma_y}{k}, \frac{d}{a}\right) \tag{7}$$

Replacing d by $(d - a)$ for convenience on the right-hand side, and adopting a series form leads to

$$\frac{1}{a}\frac{da}{dN} = \sum_i C_i\left(\frac{d-a}{a}\right)^{1-\alpha_i} \tag{8}$$

where

$$C_i = C_i\left(\frac{\Delta\sigma}{k}, \frac{E}{k}, n, \frac{\sigma_y}{k}\right)$$

However, if only the first term of the series in equation (8) is employed, the solution

$$\frac{da}{dN} = Ca^{\alpha}(d-a)^{1-\alpha} \tag{9}$$

is obtained. This crack growth equation has previously been postulated to describe the propagation of short cracks in an aluminium alloy (**7**). It can also describe the growth of cracks under elastic–plastic conditions when $\alpha = 1$, as characterized by equation (4).

Application of the short crack model

Comparing the experimental observations with equation (9), a value of d equal to the ferrite plate length seems to provide a reasonable choice, such that the propagation rate decreases on approaching the edge of the ferrite. However, in practice it was difficult to measure this dimension for each crack, so a value for d was calculated for each crack using the following method. Firstly, the values of da_s/dN were plotted (where a_s is surface crack length), as shown schematically in Fig. 5. The growth rate was calculated from the secant formula for adjacent pairs of (a, N) data, and plotted against the mean value of a over the intervening cycles (**9**). A least squares analysis was performed for those data points which showed a decrease in growth rate with increasing crack length. The point of intersection of the regression line with the abscissa in Fig. 5 gives the value of d, as equation (9) predicts zero crack growth for $a_s = d$. This

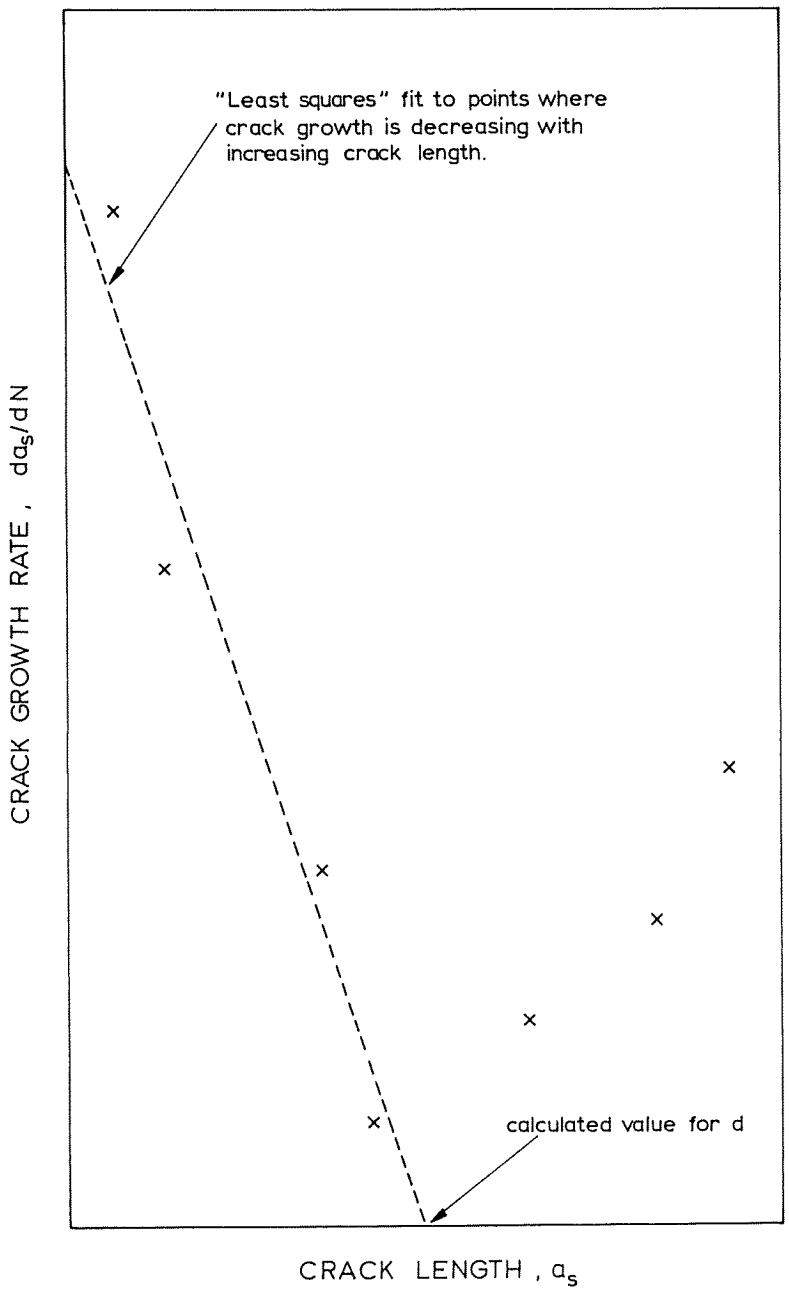

Fig 5 Schematic of calculation procedure to determine *d*

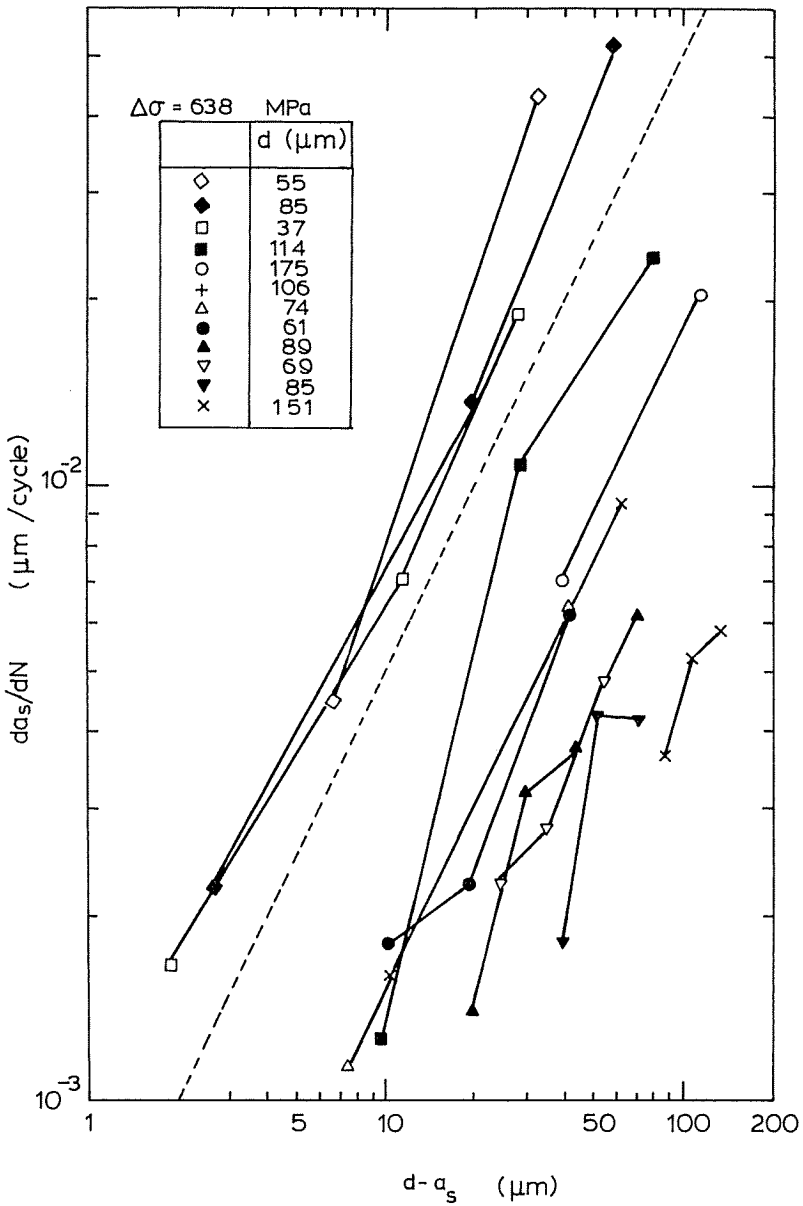

Fig 6 Observed growth rates for microstructurally short cracks

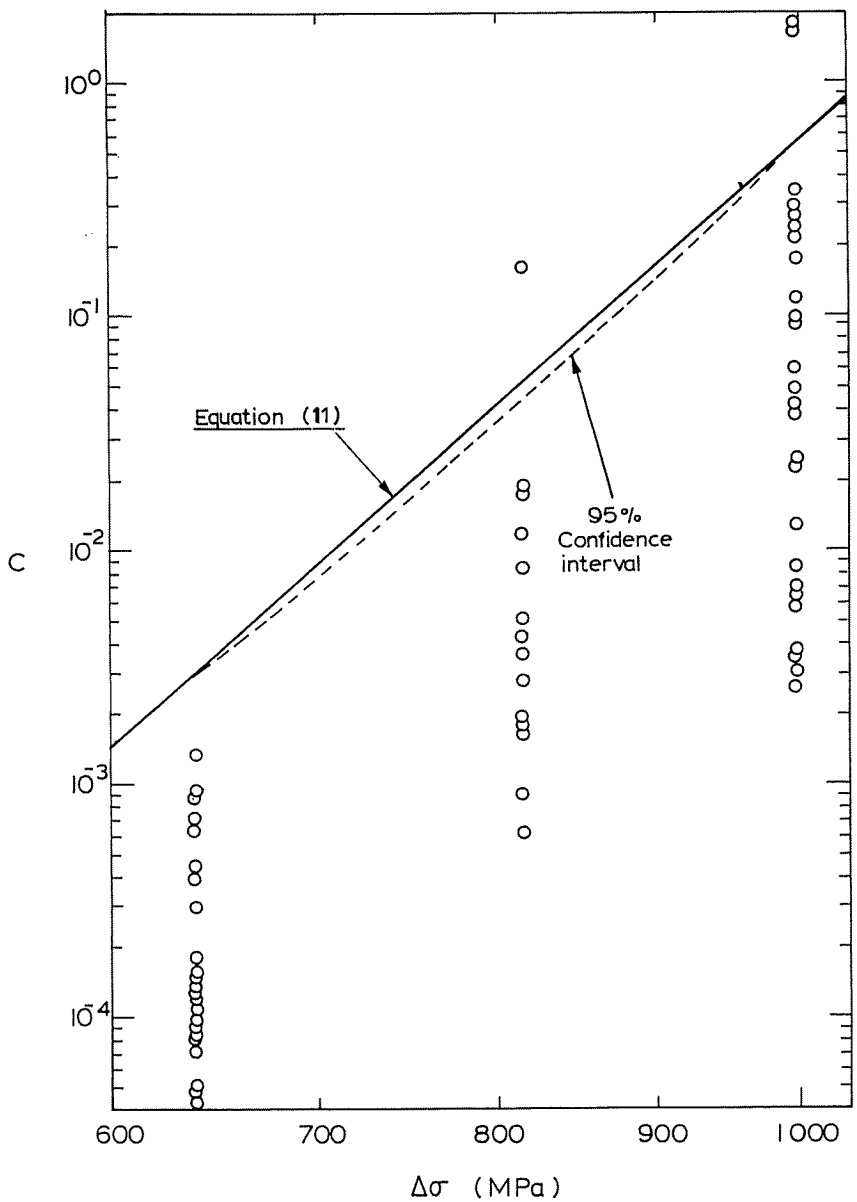

Fig 7 Dependence of the crack growth rate constant C on stress range. Dashed line shows the upper 95 per cent confidence interval

method covers the possibility that the propagation rate minimum may not correspond exactly to the instant where the crack is at the end of a ferrite plate.

In order to be of practical use, equation (9) must predict a decreasing crack growth rate as a_s approaches d. To satisfy this condition, it can be shown (**8**) that α must lie in the range $0 \leq \alpha < 1$. With a value for α of zero, equation (9) becomes, for a surface crack

$$\frac{da_s}{dN} = C(d - a_s) \tag{10}$$

Using the above calculated crack growth rate, da_s/dN, a plot of the short crack growth data for $\Delta\sigma = 638$ MPa is shown in Fig. 6, for twelve separate fatigue cracks. The dotted line represents an example of equation (10), which defines a slope of unity for lines connecting successive data points assuming $\alpha = 0$. It can be seen that this value of α defines a slope that gives a reasonable representation of microstructural short crack behaviour.

From equation (10), a value of C was calculated for every successive pair of replica data points where $a < d$. Then all these values of C were plotted against the relevant stress range, as shown in Fig. 7. This produces scatter in the values of C, but such dispersion is to be expected due to some cracks being able to propagate much more quickly than others, because of variations in the crystallographic orientations of individual grains.

It can be reasonably assumed that fast growing cracks are more likely to be the cause of final failure than those cracks which are growing slowly, so any equation expressing C as a function of stress, should take this spread of data into consideration. Therefore a 95 per cent confidence interval was taken, shown by the dotted line in Fig. 7, as being a reasonable statistical representation of the fastest observed cracks. Approximately twenty cracks were studied for each stress level, so a 95 per cent confidence interval is representative of the fastest growing crack that was measured on the replicas. Taking values for a 95 per cent confidence interval at both the lower stress of 638 MPa and the upper stress of 998 MPa, a straight line between these points is given by the equation

$$C = 1.64 \times 10^{-34}(\Delta\sigma)^{11.14} \tag{11}$$

Substituting for C into equation (10) gives

$$\frac{da_s}{dN} = 1.64 \times 10^{-34}(\Delta\sigma)^{11.14}(d - a_s) \tag{12}$$

where $\Delta\sigma$ is measured in MPa.

Continuum fracture mechanics crack growth

Crack growth data were obtained from replicas where the surface crack length (a_s) was greater than d for each of the three stress levels. An equation of the form

$$\frac{da_s}{dN} = Ga_s - D \tag{13}$$

was assumed to describe the crack growth rate where G is dependent on the stress level. This corresponds with equation (4), but with an added constant D to represent the crack growth threshold. Since equation (13) cannot accommodate microstructural influences on crack growth, a regression line was fitted to the data points obtained from replicas where the crack length was greater than 400 microns. By expressing G as a function of the total strain range, equation (13) became (**8**)

$$\frac{da_s}{dN} = 4.10(\Delta\varepsilon_t)^{2.06}a_s - D \tag{14}$$

where a_s is measured in microns.

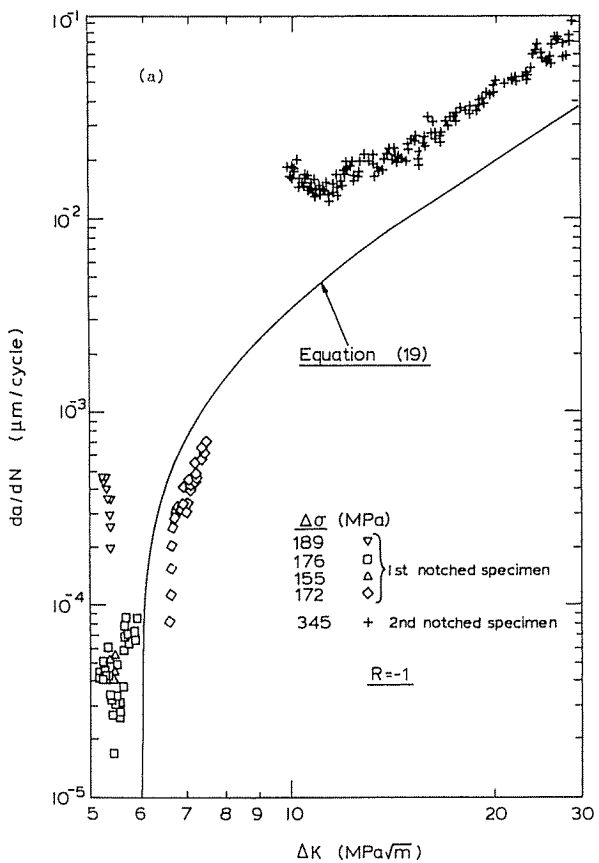

Fig 8(a) Crack growth behaviour close to threshold

To determine D, use was made of threshold data obtained on a notched specimen. These data, shown in Fig. 8(a), have an average value for ΔK_{th} of 6.0 MPa$\sqrt{m}$, where threshold is taken at a propagation rate of 10^{-10} m/cycle following the normal convention. The specimen used was of the same geometry employed in the fatigue tests, loaded in fully reversed tension–compression at a frequency of 16 Hz with a triangular waveform. Rearranging the stress intensity equation, namely

$$\Delta K = Y\,\Delta\sigma\sqrt{(\pi a)} \tag{15}$$

at threshold conditions

$$a_s = \frac{2\,\Delta K_{th}^2}{\pi Y^2\,\Delta\sigma^2} \tag{16}$$

when $a_s = 2a$, assuming a semicircular crack shape. Noting that for linear

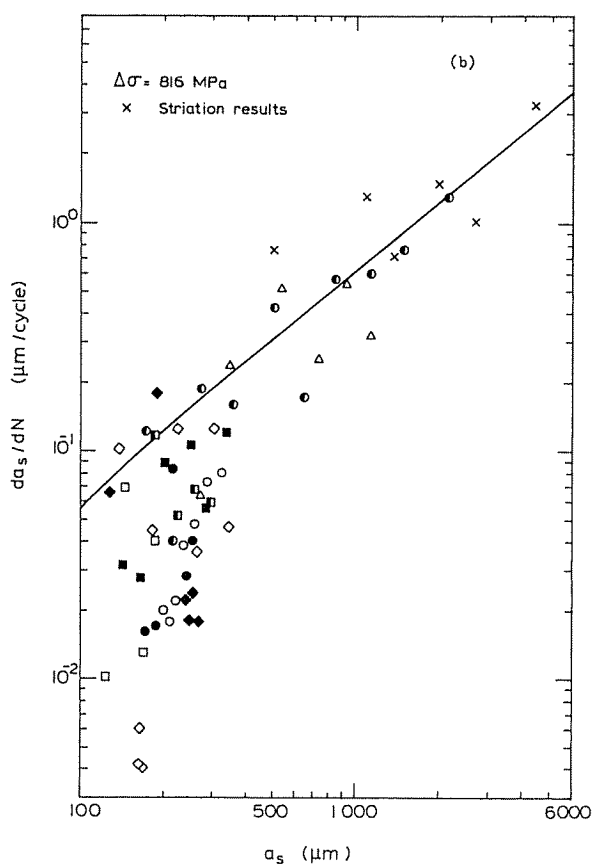

Fig 8(b) Crack growth behaviour in the low-cycle fatigue regime

elastic conditions $\Delta\sigma = E\Delta\varepsilon$, and taking $\Delta K_{th} = 6.0$ MPa$\sqrt{m}$, $Y = 2/\pi$, $E = 203$ GPa, equations (14) and (16) give for threshold conditions of zero crack growth rate

$$D = 5.63 \times 10^{-3}(\Delta\varepsilon_t)^{0.06} \quad (17)$$

Although D appears to vary with strain range, the lowest strain level used in the fatigue tests gave a value for $(\Delta\varepsilon_t)^{0.06}$ of 0.70 and the highest strain level gave $(\Delta\varepsilon_t)^{0.06}$ a value of 0.81. Thus D did not vary significantly with strain level, and an average value of $(\Delta\varepsilon_t)^{0.06}$ equal to 0.75 may be used to calculate D, giving, in equation (14)

$$\frac{da_s}{dN} = 4.10(\Delta\varepsilon_t)^{2.06}a_s - 4.24 \times 10^{-3} \quad (18)$$

which was assumed to describe crack growth for $a_s > d$ at all strain levels.

This equation is given by the line in Fig. 8(b) showing for $a_s > 400$ μm a fair fit to the data, and further justification for equation (18) is provided by the striation spacing measurements in the figure, which reflect crack growth rates on the fracture surface. Each individual crack is represented by a different symbol in this figure. By substituting for a_s in equation (18) using the relationship between a_s and ΔK in equation (15) gives

$$\frac{da}{dN} = \frac{1}{2}(1.177 \times 10^{-4}\Delta K^2 - 4.237 \times 10^{-3}) \quad (19)$$

which is also plotted in Fig. 8(a). It can be seen that the equation is an approximate fit to this low stress data, especially when considering that it is an extrapolation from tests conducted at higher strains.

Fatigue lifetime calculations

The preceding sections have shown the development of two equations, (12) and (18), to describe the rates of the respective phases of crack growth. Next it is necessary to determine the range of valid crack lengths for the application of each equation.

Equation (12) predicts crack arrest when $a = d$, which implies that the crack cannot continue propagating for $a > d$, unless equation (18) begins to contribute to crack advance. So to apply the two crack growth equations three regions of integration may be defined (7), as follows.

(*i*) *Microstructural crack zone*
This is defined to be the region where the crack grows from its initial length (assumed here to be the peak to trough surface roughness measurement R_t of 0.4 μm) to the crack length corresponding to the threshold stress intensity, a_{th}, which was calculated for each strain range by taking the value of a_s which makes da_s/dN zero in equation (18).

Table 1 Fatigue lifetime calculations

Cyclic ranges			*Threshold crack lengths*		*Calculated lifetimes (Number of cycles)*			*Calculated lifetime*	*Actual lifetime*
	Strain		*Short cracks*	*Long cracks*	*Zone 1*	*Zone 2*	*Zone 3*	*Using equations (12) and (18)*	*Using equation (3)*
Stress	*Plastic*	*Total*	d (μm)	a_{th} (μm)	*Eqn (12)*	*Eqn (12) +(18)*	*Eqn (18)*	*Number of cycles*	
MPa									
998	0.0250	0.0261	116.37	1.89	0	12	1586	1598	1254
816	0.0086	0.0138	116.37	7.08	1	97	6014	6112	6214
700	0.0039	0.0085	116.37	19.29	22	455	16907	17384	12643
638	0.0024	0.0063	116.37	35.20	122	1276	32308	33706	35778
550	0.0011	0.0039	116.37	93.41	2912	4907	113248	121067	73508

(ii) The interactive zone

This is the zone of crack growth where both the microstructural and fracture mechanics 'short' growth mechanisms, equations (12) and (18) respectively, may operate. Here the crack extends from a length a_{th} to length d, which for the purposes of integration was taken to be the average ferrite plate length observed, i.e., 116 μm.

(iii) Continuum fracture mechanics zone

This is defined to be the final region of accelerating crack growth from the end of the first ferrite plate (a = d) to the crack length at failure, a_f. A value of 4.0 mm was chosen for a_f representing half the diameter of the specimen, since for load controlled tests final fracture corresponds to a crack of such magnitude.

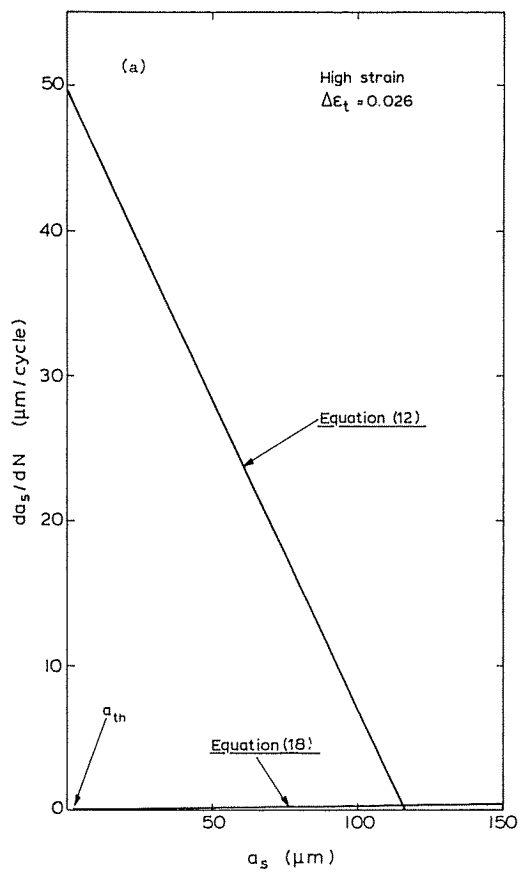

Fig 9(a) Crack growth characteristics at high strain range

By summing the three areas of crack growth the lifetime was calculated. Results of the integrations for some typical strain levels are shown in Table 1, along with the actual lifetimes obtained from equation (3). Graphs showing equations (12) and (18) for the highest and lowest strain levels are shown in Fig. 9.

It can be seen from the results of Table 1 that the calculated lifetimes are in good agreement with actual fatigue lifetimes in load controlled tests. Even for the lowest stress range, less than 2.5 per cent of the calculated lifetime is spent in region 1, suggesting that the number of cycles spent in initiating a crack may be taken as zero.

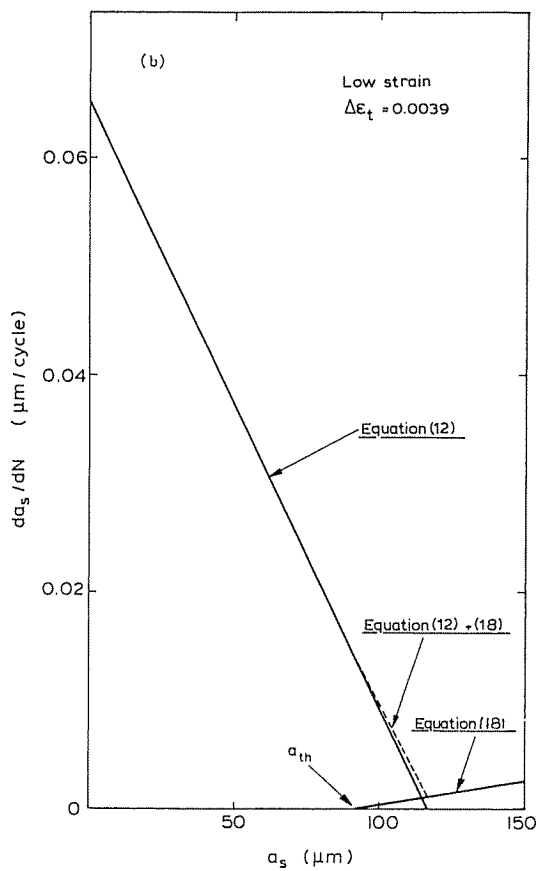

Fig 9(b) Crack growth characteristics at low strain range

Discussion

Two equations have been derived to describe the growth of cracks that are (a) short compared to dominant microstructural features, and (b) larger than those features. Equation (12) for short cracks, that is, short with respect to microstructure, shows much faster crack growth than the subsequent continuum fracture mechanics stage, described by equation (18), implying that the major proportion of lifetime is spent in propagating longer cracks, as shown in Table 1. Indeed the contribution of the initial microstructural short crack period to overall endurance is negligible, which concurs with the widely held viewpoint that low cycle fatigue can be described in terms of integrated crack propagation laws (**10**).

Having derived two equations for crack growth, and noting that no period of nucleation is required for fatigue cracks, one is in a position to attempt predictions of fatigue behaviour under variable amplitude loading. Conventionally damage is defined in terms of cycle rato (N/N_f) where N cycles are applied at a strain range corresponding to N_f cycles to failure, but the concept of damage can be replaced by a more satisfactory physical measure of damage, i.e., crack length. Indeed it has previously been demonstrated that (N/N_f) and the logarithm of crack length are directly related (**11**)(**12**). It remains, however, to include the effect of mean stress in equations (12) and (18) to obtain greater generality in the predictive capability for variable amplitude behaviour.

It is recognized that equation (12) incorporates the effect of microstructure on the simplest level through the term d. Other factors that influence crack growth should include the orientation of both the slip plane and the slip direction to the loading axis. Secondly, the representation of detailed microstructure by one dimension reflecting just a single barrier to growth is, for many microstructures, a gross simplification of actual behaviour. However, an engineering approach has been adopted in deriving equation (12), seeking to obtain an expression that is easy to apply while retaining the most important features of the growth of those cracks that eventually determine fatigue endurance.

Metallographic studies of the etched carbon steel samples showed that the values of d derived mathematically for a number of short cracks corresponded closely to the point where short cracks ran into a pearlite region. Thus, in this instance, the dominant or strong barrier to short crack growth in ferrite is provided by the ferrite/pearlite boundaries at the edges of the ferrite plates in which the cracks initiate. This conforms with the behaviour of microstructurally short cracks observed at the fatigue limit in torsional tests for the same material (**5**).

Conclusions

(1) Two equations have been derived to describe the propagation of fatigue cracks: one for microstructurally dominated short crack growth and one for elasto-plastic fracture mechanics controlled growth.

(2) The period for crack nucleation in this medium carbon steel has been shown to be negligibly small.

(3) Fatigue lifetime may be predicted by integration of the two crack growth laws, giving a good representation of the S–N curve.

(4) Pearlite provides a barrier to continued short crack propagation in a medium carbon steel where cracks form in ferrite plates.

Acknowledgements

The authors would like to thank the Central Electricity Generating Board for their sponsorship of the project, through an SERC Case Award (PDH), and a research fellowship (MWB). On of the authors (ERdlR) is also indebted to the Rio Tinto Zinc Corporation for the award of a research fellowship.

References

(1) HUNTER, M. S. and FRICK, W. M. G., Jr. (1956) Fatigue crack propagation in aluminium alloy, *Proc. ASTM*, **56**, 1038–1046.

(2) DE LANGE, R. G. (1964) Plastic replica methods applied to a study of fatigue crack propagation in steel 35CD4 and 26 SE aluminium alloy, *Trans AIME*, **230**, 644–648.

(3) LANKFORD, J. (1977) Initiation and early crack growth of fatigue cracks in high strength steels, *Engng Fracture Mech.*, **9**, 617–624.

(4) BROWN, C. W. and HICKS, M. A. (1983) A study of short fatigue crack growth behaviour in titanium alloy IMI 685, *Fatigue Engng Mater. Structures*, **6**, 67–75.

(5) DE LOS RIOS, E. R., TANG, Z., and MILLER, K. J. (1984) Short crack fatigue behaviour in a medium carbon steel, *Fatigue Engng Mater. Structures*, **7**, 97–108.

(6) LANKFORD, J. (1982) The growth of small fatigue cracks in T6-7075 aluminium alloy, *Fatigue Engng Mater. Structures*, **5**, 233–248.

(7) HOBSON, P. D. (1982) The formulation of a crack growth equation for short cracks, *Fatigue Engng Mater. Structures*, **5**, 323–327.

(8) HOBSON, P. D. (1985) *The growth of short fatigue cracks in a medium carbon steel*, PhD thesis, University of Sheffield.

(9) ASTM Standard E647-83 (1983) *Constant load amplitude fatigue crack growth rates above 10^{-8} m/cycle*, Appendix XI.

(10) WAREING, J. (1983) Mechanisms of high temperature fatigue and creep-fatigue failure in engineering materials, *Fatigue at high temperature* (Edited by R. P. Skelton) (Applied Science Publishers, London), pp. 135–185.

(11) MILLER, K. J. (1984) The propagation behaviour of short fatigue cracks, *Subcritical crack growth due to fatigue, stress corrosion and creep* (Edited by L. H. Larsson), (Elsevier Applied Science Publishers, London), pp. 151–166.

(12) MILLER, K. J. and IBRAHIM, M. F. E. (1981) Damage accumulation during initiation and short crack growth regimes, *Fatigue Engng Mater. Structures*, **4**, 263–277.